Supplementary Figures

Title: Programmed death-1 controls T cell survival by regulating oxidative metabolism

Authors: Victor Tkachev[*], Stefanie Goodell[*], Anthony W. Opipari[†], Ling-Yang Hao[‡], Luigi Franchi[‡], Gary D. Glick[§], James L.M. Ferrara[*] and Craig A. Byersdorfer[¶]

[*]Department of Pediatrics, University of Michigan, Ann Arbor, MI 48109

[†]Department of Obstetrics and Gynecology, University of Michigan, Ann Arbor, MI 48109

[‡]Lycera Corporation, 2800 Plymouth Rd, Ann Arbor, MI 48109

[§]Department of Chemistry, University of Michigan, Ann Arbor, MI 48109

¶Division of Blood and Marrow Transplant and Cellular Therapies, Department of Pediatrics, University of Pittsburgh School of Medicine, Pittsburgh PA 15224

Contents:

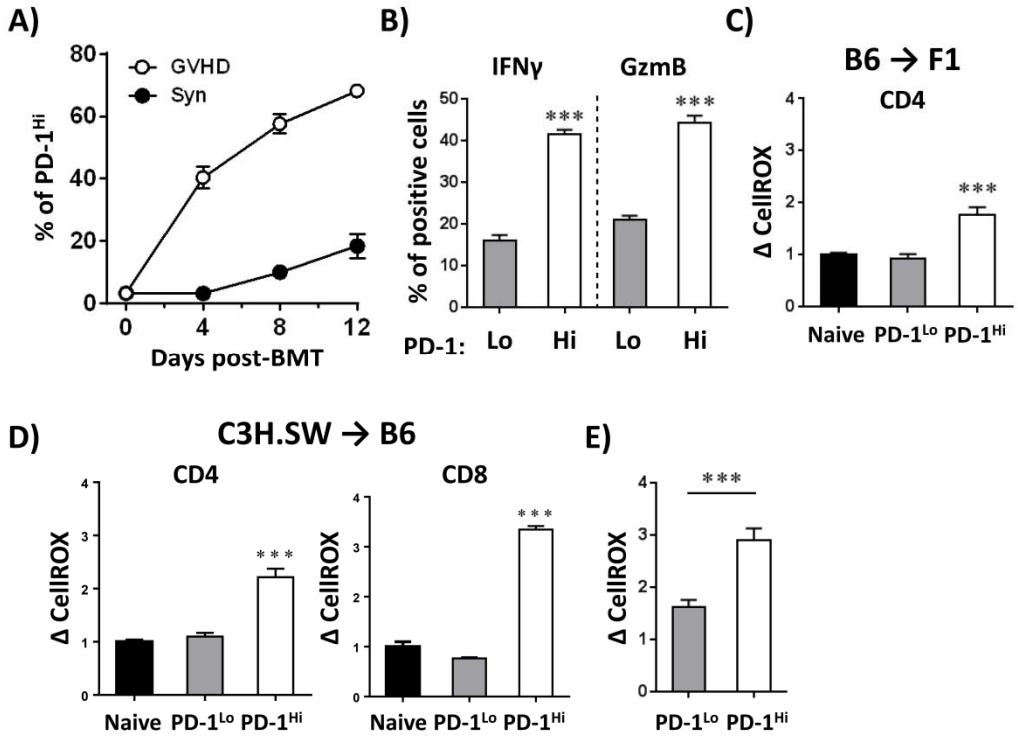

Supplementary Figure 1. Donor CD4 T cells simultaneously increase PD-1 and ROS levels post allogeneic BMT. A, B6 Ly5.2 (CD45.1$^+$) donor T cells were labeled with CellTrace and transferred to syngeneic (Syn) or allogeneic (GVHD) recipients. T cells were recovered on days 4, 8 and 12 post-BMT, stained for PD-1 and the percentage of PD-1^{Hi} cells (of total donor CD4 cells) was quantitated. Plots are gated on CD45.1$^+$, TCR-β$^+$, CD4$^+$ cells, n =4-6 mice/group. B, For IFN-γ staining, day 7 T cells were cultured for 6 hours on anti-CD3/CD28-coated plates in media containing brefeldin A, then stained for surface markers, fixed, permeabilized, and stained for intracellular IFN-γ (left panel). T cells were similarly stained for intracellular Granzyme B, only without *ex vivo* stimulation (right panel). The percentage of IFN-γ- and GzmB-positive cells was quantitated in donor CD45.1$^+$ TCR-β$^+$ CD8a$^+$ cells. C, Donor T cells were harvested as in Supplementary Figure 1A, followed by measurement of total cellular ROS. Changes in CellROX MFI in donor CD4 T cells from multiple recipients were compared to the value in un-manipulated (naïve) T cells (set to relative value of 1), n = 4-6 mice/group. D, CellTrace-labeled C3H.SW donor T cells (Ly9.1$^+$) were transferred to irradiated B6 recipients (miHC-mismatched BMT) and recovered on day 10 post-transplant. Ly9.1$^+$ TCR-β$^+$ donor cells were then stained for CD4 versus CD8, PD-1, and ROS similar to Figure 1D. CellROX MFI differences were then quantitated in well-divided PD-1^{Lo} and PD-1^{Hi} T cells from multiple recipients, n = 3-5 mice/group. E, CellROX levels in divided syngeneic T cells were determined in PD-1^{Lo} (lower left quadrant) versus PD-1^{Hi} (upper left quadrant) cells as shown in Figure 1A. In the remainder of cases, gating for PD-1^{Lo} and PD-1^{Hi} subsets was done as shown in Figure 1C. **p < 0.01, ***p < 0.001

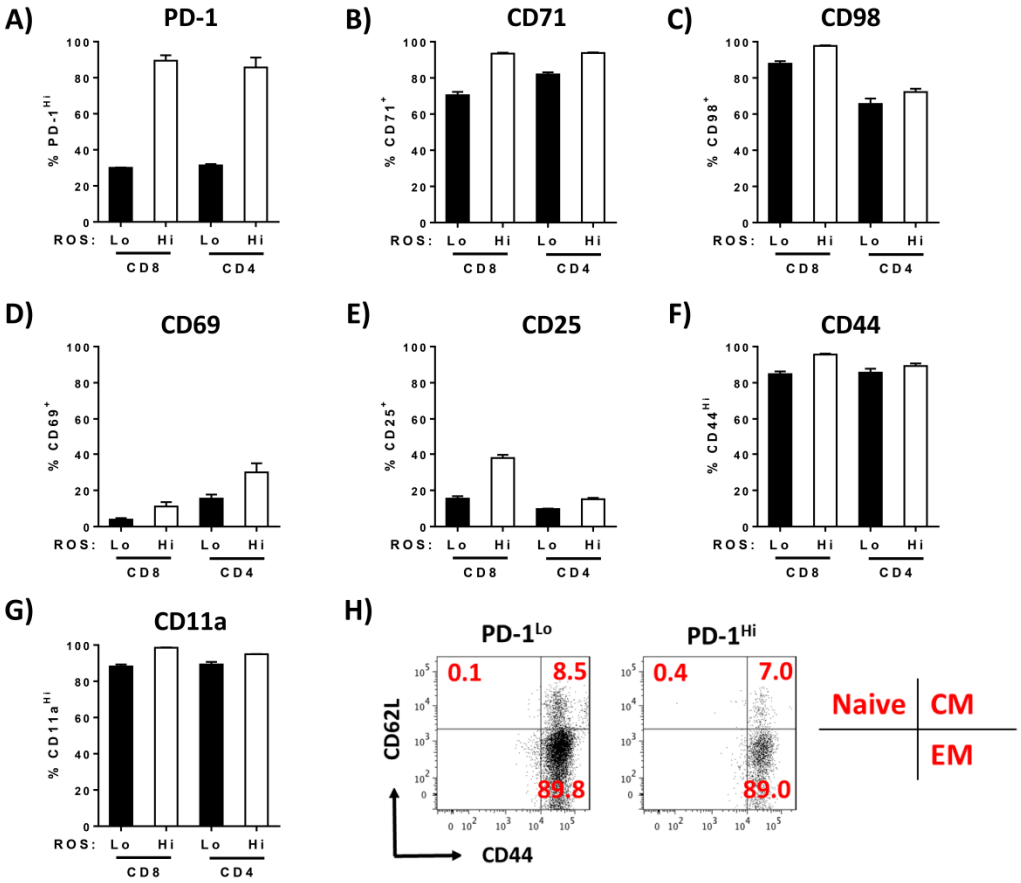

Supplementary Figure 2. In allogeneic T cells, ROS levels correlate specifically with PD-1 status. A-G, B6 Ly5.2 (CD45.1^{+}) T cells were labeled with CellTrace and transferred to irradiated, B6D2F1 allogeneic recipients. On day 7 post-BMT, donor T cells were stained for activation markers, cell surface markers, and cellular ROS levels as in Supplementary Figure 1. The percentage of CD71^{+}, CD98^{+}, CD69^{+}, CD25^{+}, CD11a^{Hi}, or CD44^{Hi} cells was then quantified in ROS ^{Lo} versus ROS^{Hi} T cells from either CD8 (left) or CD4 (right) T cell subsets. H, The percentage of cells with naïve (CD44^{Lo}CD62L^{Hi}), central-memory (CD44^{Hi}CD62L^{Hi}) and effector-memory (CD44^{Hi}CD62L^{Lo}) phenotypes was quantified in PD-1 ^{Lo} versus PD-1^{Hi} donor CD8 T cells. PD-1^{Lo} versus PD-1^{Hi} subsets were gated as shown in Figure 1C.

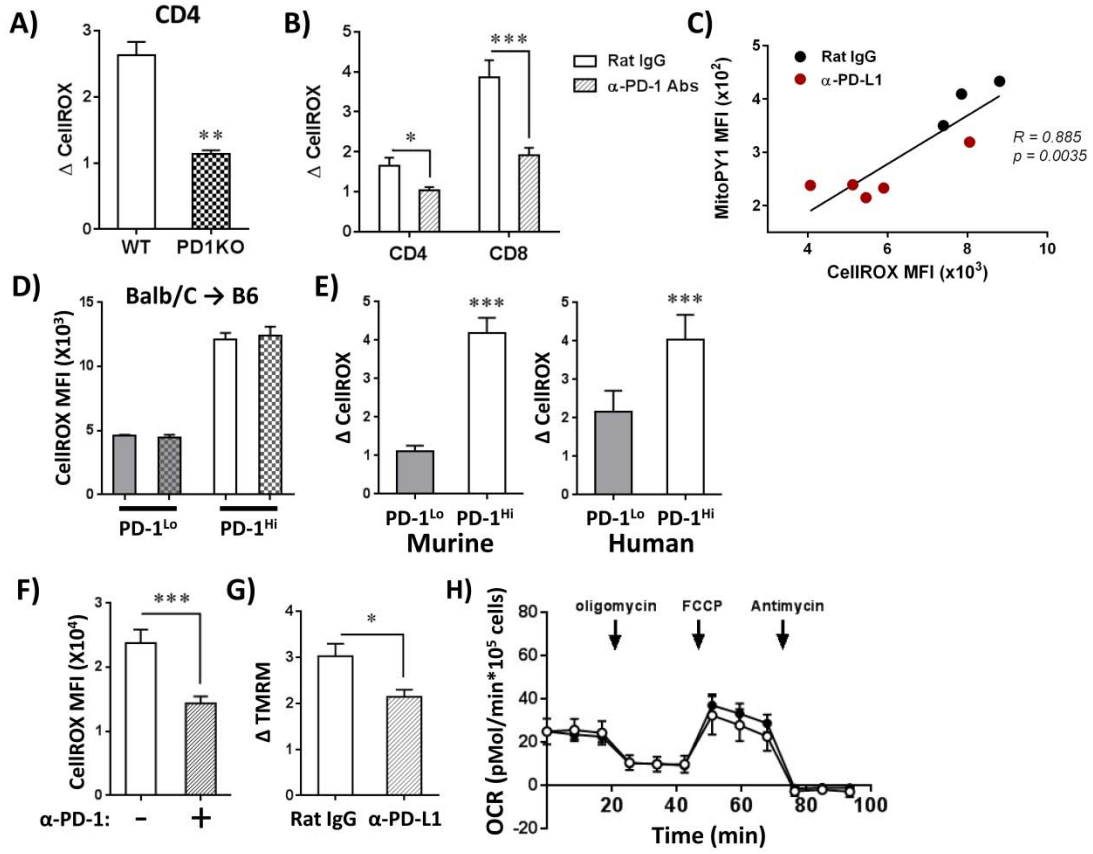

Supplementary Figure 3. PD-1 controls cellular ROS levels in murine and human alloreactive T cells. A, Wild-type (WT) or PD-1 knockout (PD-1KO) T cells were transferred to B6D2F1 recipients and changes in CellROX MFI measured day on 7 post-BMT in $CD4^+$ WT $PD\text{-}1^{Hi}$ versus PD-1KO T cells, n = 3-5 mice/group. B, B6 into F1 recipient mice were treated with anti-PD-1 blocking antibodies (or Rat IgG control) and ROS levels measured on day 7 in donor $PD\text{-}1^{Hi}$ CD4 and CD8 T cells. Staining and gating similar to Figure 2D, n = 3-5 mice/group. C, B6 into B6D2F1 recipients were treated with anti-PD-L1 blocking antibodies, followed on day 7 by simultaneous measurement of total cellular ROS (CellROX) and mitochondrial H_2O_2 (MitoPY1) in donor, $PD\text{-}1^{Hi}$, CD8 T cells. Linear regression between CellROX and MitoPy1 was then calculated, n = 3-5 mice/group. D, CFSE-labeled Balb/C T cells were transplanted into irradiated WT (solid) or PD-L1KO (hatched) recipients. Donor T cells were recovered on day 5 post-BMT and assessed for cellular ROS in $PD\text{-}1^{Lo}$ versus $PD\text{-}1^{Hi}$ T cells, n = 3-4/group. $PD\text{-}1^{Lo}$ versus $PD\text{-}1^{Hi}$ subset gating as performed similar to Figure 1C. E, Murine and human T cells were plated in MLRs (outlined in Figure 3) and harvested on day 4 (murine) or day 6 (human). PD-1 expression and ROS levels were then measured in $PD\text{-}1^{Lo}$ (left lower quadrant) versus $PD\text{-}1^{Hi}$ (left upper quadrant) $CD4^+$ T cells. F, Human MLR cultures were treated with anti-PD-1 antibodies on days 0, 3, and 6. Eight hours after the final treatment, ROS levels were measured in $CD4^+$, $PD\text{-}1^{Hi}$ cells; n = 8 independent human samples. G, B6 into F1 recipients were treated with anti-PD-L1 antibodies (or Rat IgG control) as in Figure 2C. On day 7 post-transplant, mitochondrial transmembrane potential was measured in donor $CD8^+$ T cells. H, BMT and treatment as in Figure 4A (solid circles = anti-PD-L1 antibodies, open circles = Rat IgG control). On Day 7 post-BMT, donor T cells were isolated, pretreated with 100 μM Etomoxir for 15 minutes, and applied to Seahorse XF24 analyzer to measure oxygen consumption rates (OCR). *p<0.05, **p<0.01, ***p<0.001

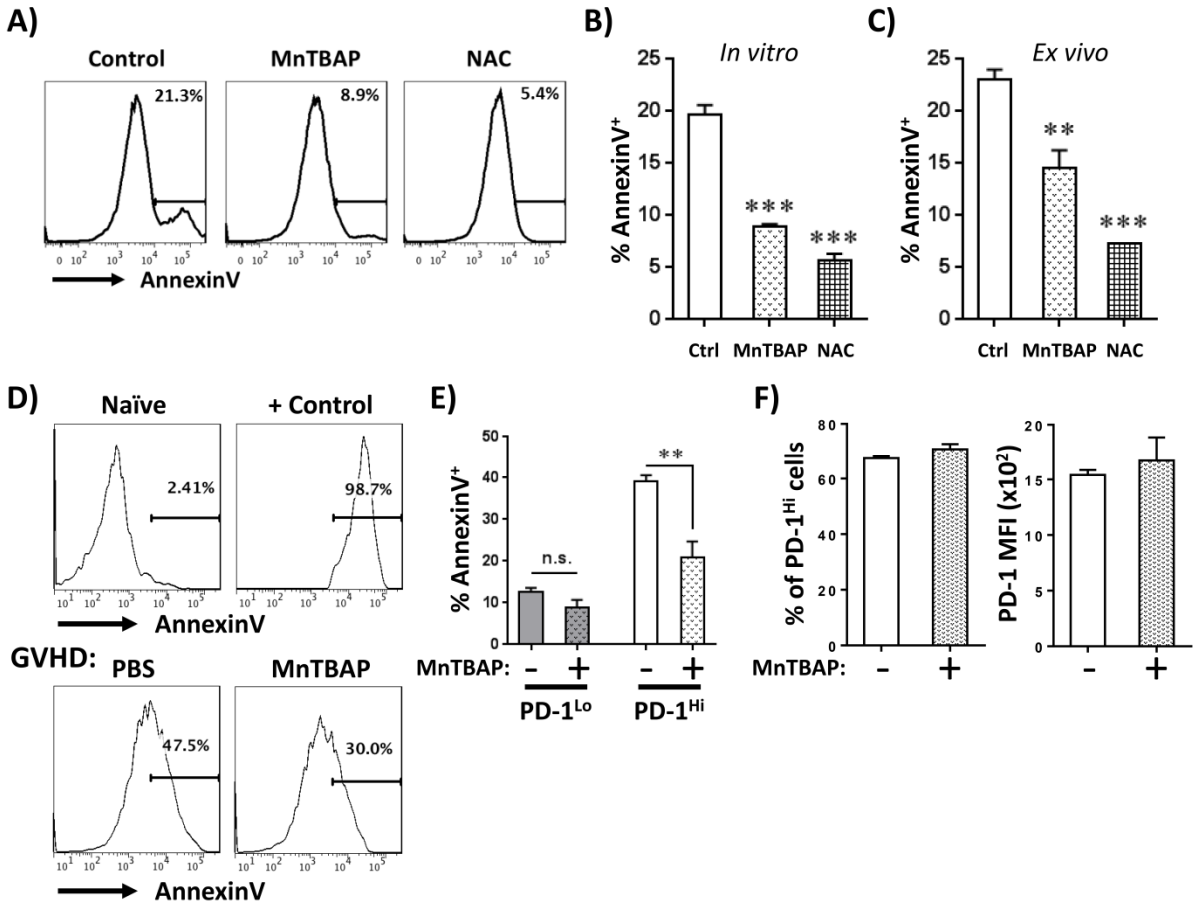

Supplementary Figure 4. Antioxidants protect PD-1^{Hi} T cells from apoptosis. A, OT-I T cells were stimulated *in vitro* with CAG-OVA splenocytes as detailed in Materials and Methods. Anti-oxidant compounds MnTBAP (100 μM) or NAC (10 mM) were added at 48 hours, cells harvested the following day, and donor T cells (CD45.2^{+}TCRβ^{+}CD8^{+}) stained for AnnexinV. B, The percentage of AnnexinV^{+} cells was quantified in TCRβ^{+}CD8^{+} OT-I cells from multiple replicates, n = 5 donors/group. C, Donor T cells from B6 into B6D2F1 recipients were purified on day 7 post-BMT and plated with B6D2F1 splenocytes for 24 hours. MnTBAP (100 μM) or NAC (10 mM) were added at the time of re-stimulation. After 24 hours, donor T cells were stained for surface markers and AnnexinV as in Supplementary Figure 4B. The percentage of AnnexinV^{+} cells was then quantitated in donor PD-1^{Hi} CD8 T cells. PD-1^{Hi} subset gated as in Figure 1C, n = 5 recipient mice/group. D, B6 into B6D2F1 recipients were treated with PBS or MnTBAP on day 7 post-BMT, donor cells recovered the following day, and donor CD4 or CD8 T cells (CD45.1^{+}, TCR-β^{+}) stained for PD-1 and AnnexinV. E, The percentage of AnnexinV^{+} cells in donor PD-1^{Lo} or PD-1^{Hi} CD4 T cells was quantitated from multiple recipients, per primary data in Supplementary Figure 4D. F, Cells were harvested and stained similar to Figure 5C. Graphs represent the percentage of PD-1^{Hi} T cells (left) or the MFI of PD-1 staining (right) on donor CD8 T cells from multiple recipients, n = 5 mice/group. *$p < 0.05$, **$p < 0.01$, ***$p < 0.001$